LECTURE 5

[44] J.E.Bayfield and P.M.Koch, Phys. Rev. Lett., v.33, p.258 (1974) [first experiment of quantum chaos, hydrogen in microwave field].

[45] N.B.Delone, B.A.Zon and V.P.Krainov, ZETP v.75, N 2(6), p.445 (1978) [diffusive mechanism of ionization].

[46] J.D.Leopold and I.C.Percival, Phys. Rev. Lett. v.41, p.944 (1978) [classical numerical simulations, agreement with experiment].

[47] B.I.Meerson, E.A.Oks and P.V.Sasorov., Pis'ma ZETP, v.29, p.79 (1979) [estimate for chaos border near $\omega_0 \approx 1$].

[48] R.V.Jensen, Phys. Rev. Lett., v.49, p.1365 (1982) [1-dimensional model].

[49] N.B.Delone, V.P.Krainov, D.L.Shepelyansky, "Highly excited Atom in Electromagnetic Field", Usp. Fiz. Nauk v.140, p.355-392 (1983) [Sov. Phys. Uspekhy v.26, p.551 (1983)] [1-dimensional model, chaos border as function of frequency, diffusion rate dependence on frequency].

[50] D.L.Shepelyansky, "Quantum Diffusion Limitation at Excitation of Rydberg Atom in Variable Field", Preprint INP 83-61 (Novosibirsk 1983); Proc. Int. Conf. on Quantum Chaos (Como 1983), Ed. G.Casati, Plenum p.187 (1985) [first quantum simulations, quantum localization of classical diffution, first analytical estimates].

[51] G.Casati, B.V.Chirikov, D.L.Shepelyansky, "Quantum Limitations for Chaotic Excitation of Hydrogen Atom in Monochromatic Field", Phys. Rev. Lett. v.53, p.2525-2528 (1984) [dependence of localization length on parameters].

[52] K.A.H Van Leeuwen, G.V.Oppen, S.Renwick, J.B.Bowlin, P.M.Koch, R.V.Jensen, O.Rath, D.Richards, J.G.Leopold, Phys. Rev. Lett., v.55, p.2231 (1985) [excellent agreement between classical simulations and experiment].

[53] G.Casati, B.V.Chirikov, I.Guarneri,D.L.Shepelyansky, "Relevance of Classical Chaos in Quantum Mechanics: the Hydrogen Atom in a Monochromatic Field", Phys. Rep. v.154, p.77-123 (1987) [localization, diffusive photoelectric effect, time reversability in microwave ionization].

[54] R.Blumel and U.Smilansky, Z. Phys. D, v.6, p.83 (1987) [microwave ionization, $\omega_0 < 1$].

[55] G.Casati, I.Guarneri, D.L.Shepelyansky, "Hydrogen Atom in Monochromatic Field: Chaos and Dynamical Photonic Localization", IEEE Jour. of Quant. Elect. v.24, p.1420-1444 (1988) [classical/quantum Kepler map, photonic localization, explanation of localization in 2d-hydrogen, modern theory].

[56] E.J.Galvez, B.E.Sauer, L.Moorman, P.M.Koch and D.Richards, Phys. Rev. Lett., v.61, p.2011 (1988) [observation of dynamical localization in microwave ionization of hydrogen].

[57] J.E.Bayfield, G.Casati, I.Guarneri and D.W.Sokol, Phys. Rev. Lett., v.63, p.364 (1989) [observation of dynamical localization in microwave ionization of hydrogen].

[58] G.Casati, I.Guarneri, D.L.Shepelyansky, "Classical Chaos, Quantum Localization and Fluctuations: a Unified View", Physica v.163A, p.205 (1990) [quantum Kepler map despription of Koch experiment ref.56].

[59] M.Arndt, A.Buchleitner, R.N.Mantegna and H.Walther, Phys. Rev. Lett., v.67, p.2435 (1991) [observation of dynamical localization in microwave ionization of Rb].

[60] R.V.Jensen, S.M.Suskind and M.M.Sanders, Phys. Rep. v.201, p.1 (1991) [review of experimental and theoretical situation in microwave ionization].

[61] A.Buchleitner and D.Delande, Phys. Rev. Lett., v.70, p.33 (1993) [complex rotation method for microwave ionization].

[62] D.L.Shepelyansky, "Dynamical Localization in Hydrogen Atom", Lectures at Enrico

Fermi Summer School "Quantum Chaos", Varenna 1991, in Quantum Chaos, Eds. G.Casati, I.Guarneri, U.Smilansky, North-Holland, Amsterdam, pp.221-240, 1993.

[63] A.A.Konovalenko, Pis'ma v astron. Zhurnal, v.10, N11, p.846 (1984); ibid, v.10, N 12, p.912 (1984) [Rydberg atoms in space, n=732].

[64] J. Neukammer, H.Rinneberg, K.Vietzke, A.Konig, H.Hieronymus, M.Kohl, H.-J.Grabka, G.Wunner, Phys. Rev. Lett., v.59, p.2947 (1987) [Rydberg atoms in lab, n=550].

(34a)

# Hydrogen atom in a microwave field

## Twenty years after

A. Duma

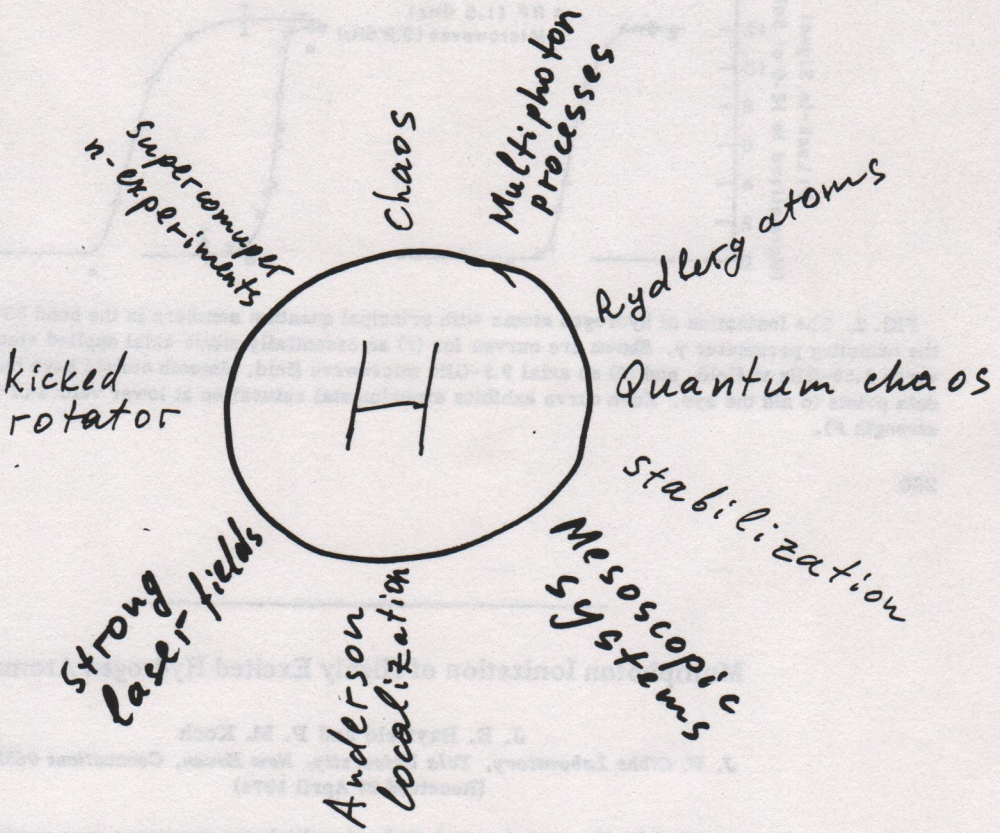


(≈20)

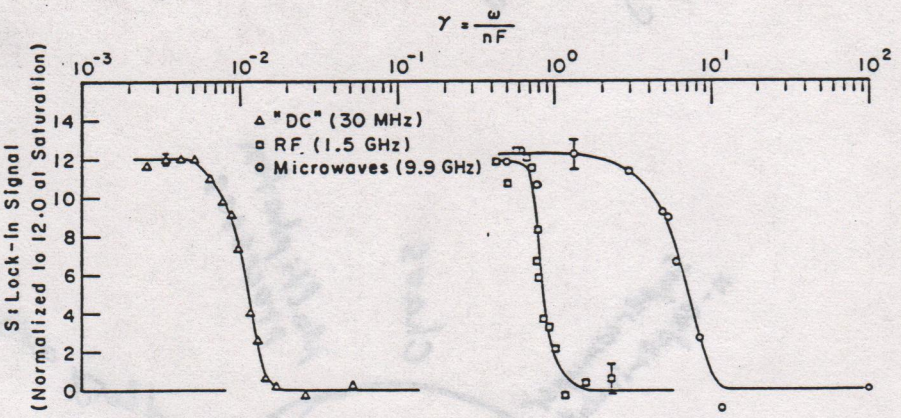


FIG. 2. The ionization of hydrogen atoms with principal quantum numbers in the band $63 \leq n \leq 69$, as a function of the tunneling parameter $\gamma$. Shown are curves for (1) an essentially static axial applied electric field, (2) a transverse 1.50-GHz rf field, and (3) an axial 9.9-GHz microwave field. Smooth curves have been drawn through the data points to aid the eye. Each curve exhibits experimental saturation at lower values of $\gamma$ (higher values of field strength $F$).

260

## Multiphoton Ionization of Highly Excited Hydrogen Atoms*

J. E. Bayfield and P. M. Koch
*J. W. Gibbs Laboratory, Yale University, New Haven, Connecticut 06520*
(Received 29 April 1974)

A new method for the experimental study of multiphoton processes uses production of highly excited atoms in keV electron-transfer collisions. Such atoms can be ionized over a wide range of frequencies of an external electromagnetic field, permitting studies of multiphoton-ionization processes for regimes not yet achieved in laser experiments. Results for microwave ionization of hydrogen atoms with principal quantum numbers in the band $63 \leq n \leq 69$ are discussed in terms of the available theory.

(F20)

The multiphoton ionization of atoms by intense oscillating electromagnetic fields is not well understood at present. Theoretical interpretation of laser-ionization experiments has treated the electric field $F\cos(\omega t)$ as a perturbing influence on the electronic motion within the atom, under conditions where the field oscillates rapidly with a period $T$ short compared to the time of flight $\tau$ of the electron to a distance $r_0$ where the external field $F$ would dominate over the attractive force $F_0$ of the atomic nucleus. However, when pulsed lasers of greater power become available for experiments on ground-state atoms, new regimes will be reached where either or both of the conditions $F \ll F_0$ and $T \ll \tau$ becomes inapplicable. It is the purpose of this paper to demonstrate that experiments within these new regimes can be done now by lowering the frequency into the microwave region to give larger $T$ while reducing the field strengths required by using highly ex-

258

(70)

$\frac{\Gamma_D}{\Gamma_1} \sim n_0^{4/3}/16$

Casati
Chirikov
Guarneri
Shepelyansky
(1986)

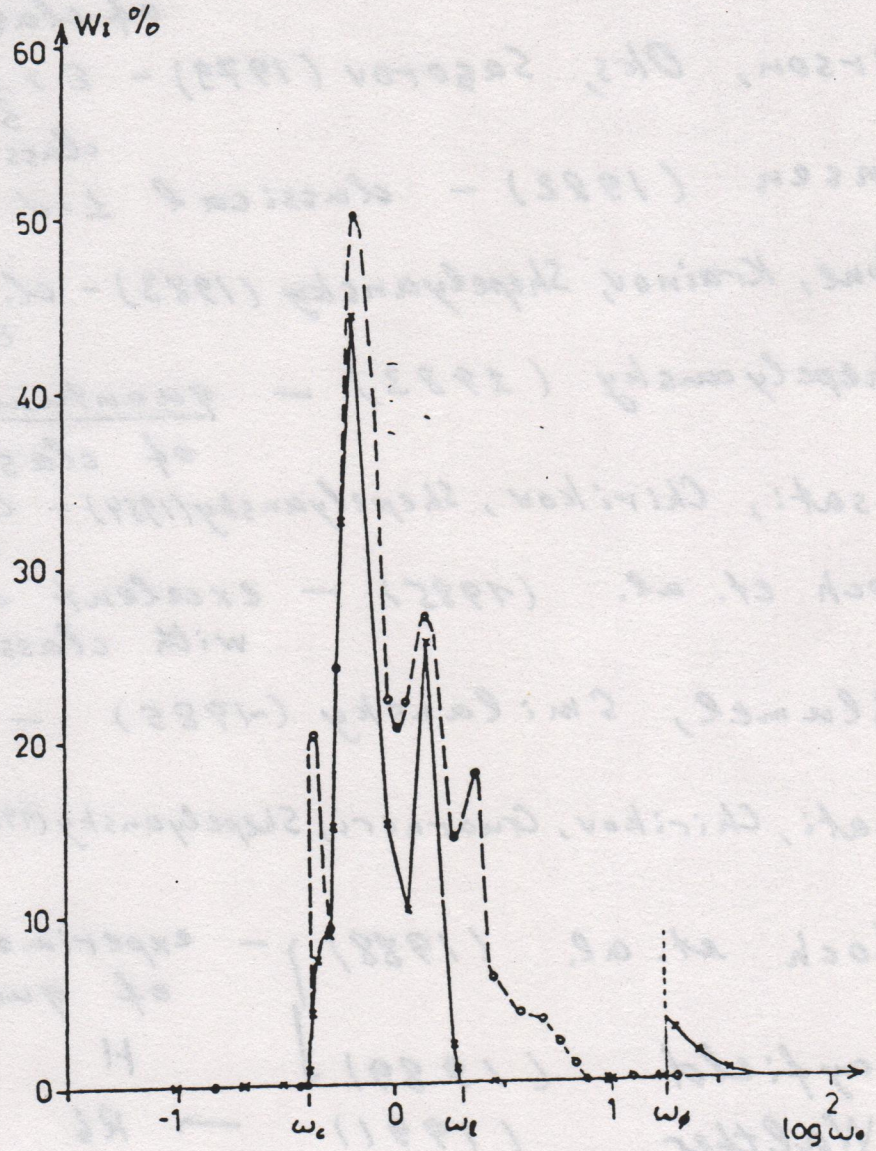


$n_0 = 66$

$\varepsilon_0 = 0.05 =$
$= 13.5 V/cm$

$\Delta t = 40 \omega_0 \frac{2\pi}{}$

$\approx 1.7 \cdot 10^{-9}$ s

$\omega_0 = 1 \rightarrow 23 GHz$

Ionization probability as a function of frequency $\omega_0 = \omega n_0^3$.

Interaction time
$\Delta t \approx 1.7 \cdot 10^{-9}$ s

x - quantum

o - classical

$\omega_\phi$ is one-photon ionization border

*Рис. 18.* Зависимость вероятности ионизации $W_l = \sum_{n > n^*} |C_n|^2$ от частоты поля $\omega_0$ после $\tau = 40\omega_0$ периодов поля, что соответствует одному и тому же физическому времени $t$ для всех частот.

Здесь $n_0 = 66$, $\varepsilon_0 = 0.05$, $n^* = 99$, * — квантовые численные данные. O — классические. Значение однофотонной границы $\omega_\phi$ несколько меньше $n_0/2$ из-за конечности $n^*$.



(F21)

(35) Bayfield, Koch (1974, 1977, ... 1994)

Delone, Zon, Krainov (1978) – diffusion in energy, ionization time estimate $\varepsilon_{cr} > 1/n^5$

Leopold, Percival (1978) – numerical simulations of classical equations

Meerson, Oks, Sagorov (1979) – $\varepsilon > \frac{1}{30n^4}$, $\omega_0 \sim 1$ classical chaos border

Jensen (1982) – classical 1-d model

Delone, Krainov, Shepelyansky (1983) – cl. 1-d. model $\varepsilon_0 > \frac{1}{49\omega_0^{4/3}}$; $D(\omega)$

Shepelyansky (1983) – quantum suppression of classical chaos

Casati, Chirikov, Shepelyansky (1984) – localization length

Koch et. al. (1985) – excelent agreement with classical dynamics

Blumel, Smilansky (~1985) – $\omega_0 < 1$ bumps

Casati, Chirikov, Guarneri, Shepelyansky (1986-88) – $l_\varphi$, Keplep map 2D

Koch et. al. (1988) } – experimental observati: of quantum localiza

Bayfield (1989) } H

Walther (1991) → Rb

. . . . . .

Buchleitner, Delande (1993) – quantum localiza tion, new numeri- cal methods

From 1992 - 93 → Rydberg stabilizatio

# Hydrogen atom in microwave field



Bayfield, Koch experiment (1974)

H - principal quantum number

$$n \sim 70, \quad \mathcal{E} \sim 10\ V/cm, \quad \frac{\omega}{2\pi} \approx 10\ GHz$$

$$E_n = -\frac{1}{2n^2} \quad (a.u.) \quad \left(\sim \frac{1}{r}, \ r \sim n^2\right)$$

$$\Delta = E_{n+1} - E_n = \frac{1}{n^3} \longrightarrow \omega n_0^3 = \omega_0$$

$$V = \mathcal{E} z \sim \mathcal{E} n^2 \sim E_n \sim \frac{1}{n^2} \longrightarrow \mathcal{E} n_0^4 = \mathcal{E}_0$$

$n_0 = 100$
$\omega_0 = 1.519 \rightarrow 10\,GHz$
$\mathcal{E}_0 = 0.1 \rightarrow \mathcal{E} = 5.14\ \frac{V}{cm}$

In experiment: $\omega_0 \approx 0.43$, $\mathcal{E}_0 \sim 0.05$

$$N_I = \frac{1}{2n_0^2 \omega} = \frac{n_0}{2\omega_0} \sim 100 \quad \text{(number of photons)}$$

(F21)

$\mathcal{E}_{st\,0} \approx 0.13$

---

Other experiments

| | | | |
|---|---|---|---|
| H | Bayfield | (Pittsburg) | $n \lesssim 90$ |
| H | Koch | (Stony Brook) | |
| Rb | Walther | (Munich) | $n \sim 150$ |
| -"- | Rinneberg | (Berlin) | $n \approx 550$ |

---

In space

| | | | |
|---|---|---|---|
| C | Konovalenko | (Kharkov) | $n = 732$ |

# Classical Dynamics

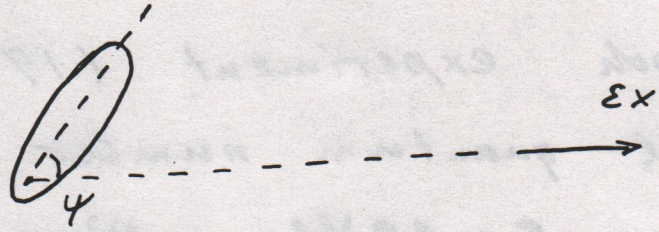


$$H = \frac{p_x^2 + p_y^2}{2} - \frac{1}{(x^2+y^2)^{1/2}} + \varepsilon x \cos\omega t$$

$$H = -\frac{1}{2n^2} + \varepsilon n^2 \cos\omega t \left[\cos\psi \left\{\frac{3}{2} e - 2\sum_{s=1}^{\infty} x_s \cos(s\theta)\right\} + \right.$$
$$\left. + \sin\psi \left\{2\sum_{s=1}^{\infty} y_s \sin(s\theta)\right\}\right]$$

$(n,\theta)$, $(l,\psi)$ – canonical variables

$e = \sqrt{1 - l^2/n^2}$ – eccentricity

Landau, Lifshitz II

$$x_s = J_s'(se)/s, \quad y_s = (1-e^2)^{1/2} J_s(se)/se$$

$\omega_0 = \omega n_0^3 > 1$ $\quad (s \approx \omega_0 \gg 1)$ $\quad \Phi$ – Airy function

Resonant condition: $s\dot\theta = \omega \Rightarrow s = \omega n_s^3$.

$$J_s(se) \approx \frac{1}{\sqrt{\pi}} \left(\frac{2}{s}\right)^{1/3} \Phi\left(\left[\left(\frac{s}{2}\right)^{2/3}(1-e^2)\right]\right) \approx$$

$$\approx \frac{1}{\sqrt{\pi}} \left(\frac{2}{\omega n^3}\right)^{1/3} \Phi\left(\left(\frac{\omega}{2}\right)^{2/3} l^2\right)$$

$$l < l_c \approx \left(\frac{3}{\omega}\right)^{1/3}$$

Extended orbits: $e = \left(1 - \frac{l^2}{n^2}\right)^{1/2} \approx 1$

$$y_s \approx \frac{l}{n} \frac{J_s(s)}{s} \approx \frac{2^{1/3}}{\sqrt{\pi}} \frac{l}{n} \frac{\Phi(0)}{s^{4/3}} \approx 0.447 \frac{l}{n} \frac{1}{s^{4/3}}$$

$$x_s = \frac{1}{s} \frac{1}{s} \frac{\partial}{\partial e} J_s(se)\Big|_{e=1} \approx -\frac{2^{2/3}}{\sqrt{\pi}} \frac{\Phi'(0)}{s^{5/3}} \approx \frac{0.411}{s^{5/3}} \left(1 + \frac{l^2}{2n^2}\right.$$

(38)

# One-dimensional model ($\psi = 0$)

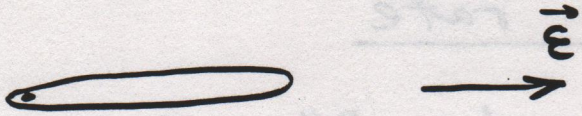


$$H = -\frac{1}{2n^2} + \varepsilon n^2 \cos\omega t \left[\frac{3}{2} - 2\sum_{s=1}^{\infty} x_s \cos(s\theta)\right]$$

$$\omega = s\dot{\theta} = s n_s^{-3} = s\Omega_s \quad ; \quad n_s = \omega/s$$

Resonant Hamiltonian near resonance $s$:

$$H_s = -\frac{3}{2}\frac{(n-n_s)^2}{n_s^4} - \varepsilon n_s^2 x_s \cos(s\lambda)$$

Pendulum

$\frac{H''(\Delta n)^2}{2}$

$\lambda = \theta - \frac{\omega}{s} t$ Separatrix $\rightarrow H_s = -\varepsilon n_s^2$

Half width in action

$$\Delta n = \left[\frac{2n_s^4}{3}\varepsilon n_s^2 x_s \cdot 2 \cdot \underbrace{\sin^2\left(\frac{s\lambda}{2}\right)}_{=1}\right]^{1/2} = \frac{2}{\sqrt{3}} n_s^2 \sqrt{\varepsilon x_s}$$

Half width in frequency

$$\Delta\Omega_s = \frac{3\Delta n}{n_s^4} = \frac{2}{n_s}\sqrt{3\varepsilon x_s}$$

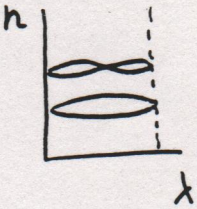


Overlapping of resonances:

$$S = \frac{\Delta\Omega_s + \Delta\Omega_{s+1}}{\Omega_s - \Omega_{s+1}} \quad ; \quad \Omega_s - \Omega_{s+1} \approx \frac{\omega}{s^2}$$

$$\Delta\Omega_s = \frac{2}{n_s}\left[\frac{3\cdot 0.411}{s^{5/3}}\varepsilon\right]^{1/2} \approx \Delta\Omega_{s+1}$$

Global chaos: $K = 2.5\, S^2 > 1$

$$K = 2.5 \cdot \frac{16\cdot 3\cdot 0.411\cdot \varepsilon s^4}{n_s^2 s^{5/3}\omega^2} \approx 49(\varepsilon n_s^4) s^{1/3} = 49\varepsilon_0 \omega_0^{1/3} > 1$$

$$\varepsilon_0 > \varepsilon_c = \frac{1}{49\omega_0^{1/3}} \quad ; \quad \varepsilon n^4 > \frac{1}{49\omega^{1/3} n}$$

(39)

# Diffusion rate

$$D_t = \pi \frac{F_0^2}{\Delta_0}; \qquad \dot{n} = -\frac{\partial H}{\partial \theta} = -\sum_s \varepsilon n_s^2 s x_s \sin(s\lambda)$$

$$\Delta_0 = \dot{\theta} = n_s^{-3} \qquad s\lambda = s\theta - \omega t.$$

$$F_0 = \varepsilon n_s^2 x_s s; \quad \Delta_0 = n_s^{-3}; \quad x_s = 0.411/s^{5/3}; \quad s = \omega_k^3$$

$$D_t = 0.530 \cdot \frac{\varepsilon^2 n_s^7}{s^{4/3}} = 0.530 \cdot \frac{\varepsilon^2 n^3}{\omega^{4/3}} \quad - \text{per unit of time}$$

$$D_n = \frac{(\Delta n)^2}{\Delta t} = 2\pi D_t/\omega = 3.33 \frac{\varepsilon^2 n^3}{\omega^{7/3}} \quad - \text{per field period}$$

Diffusion rate in number of photons per orbital period:

$$D = D_t \cdot 2\pi n^3 \cdot \left(\frac{dE_n}{dn}\right)^2 \frac{1}{\omega^2} = \frac{(\Delta N)^2}{\text{orbital period}}$$

$$N = E/\omega$$

$$D = 3.33 \frac{\varepsilon^2}{\omega^{10/3}}$$

(a)

## Fokker - Plank description

Ionization time $\Delta n \sim n_0$

$$\tau_I \sim \frac{n_0^2}{D_{n_0}} \sim \frac{\omega_0^{7/3}}{\varepsilon_0^2} \gg 1$$

FPK - equation

$$\frac{\partial f}{\partial \tau} = \frac{1}{2} \frac{\partial}{\partial n} \left( D_n \frac{\partial f}{\partial n} \right)$$

New variables $y = n/n_0$, $\bar{\tau} = D\tau$

$$G(y, \bar{\tau}; y_0) = \frac{z z_0}{\sqrt{y y_0}} e^{-(z^2 + z_0^2)} I_{\pm 2}(2 z z_0)$$

$$z = \frac{1}{\sqrt{y \bar{\tau}}}; \quad z_0 = \frac{1}{\sqrt{y_0 \bar{\tau}}}; \quad y_0 = 1$$

For $\bar{\tau} \ll 1$, $z \gg 1 \Rightarrow I_p(x) \approx e^x / \sqrt{2\pi x}$,

for $\bar{\tau} \sqrt{y} \ll 1$

$$f(y, \bar{\tau}) = \frac{\exp\left[ -\left( 1/\sqrt{y} - 2/\sqrt{\bar{\tau}} + 1 \right)^2 / \bar{\tau} \right]}{2 y^{3/4} \sqrt{\pi \bar{\tau}}} +$$

$$+ \frac{\exp\left[ -\left( 1/\sqrt{y} - 1 \right)^2 / \bar{\tau} \right]}{2 y^{3/4} \sqrt{\pi \bar{\tau}}}$$

$\bar{y} = \bar{n}/n_0$

$\left. \frac{\partial f}{\partial n} \right|_{\bar{n}} = 0$

(40)

# Derivation of Kepler map

$$H = -\frac{1}{2n^2} + \varepsilon X(\theta)\cos\omega t$$

For Kepler motion (eccentric anomaly $\xi$)

$$X = n^2(1-\cos\xi)$$

$$t = n^3(\xi - \sin\xi) + \varphi$$

$$\theta = \xi - \sin\xi$$

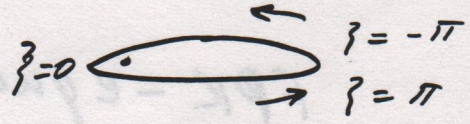


$\xi = \xi(\theta)$ ; $dt = n^3 d\theta$

$$\dot{n} = -\frac{\partial H}{\partial \theta} = -\varepsilon n^2 \cos\omega t \sin\xi \frac{d\xi}{d\theta}$$

$$\Delta n = \int_{\text{orb.period}} dt\left(-\frac{\partial H}{\partial \theta}\right) =$$

$$= -\varepsilon n^5 \int_{-\pi}^{\pi} d\xi \cos\underbrace{\underbrace{\left(\varkappa(\xi-\sin\xi)+\phi\right)}_{\omega t}}_{\omega n^3} \sin\xi =$$

($\omega t$: field phase at perihelion; $\omega n^3$: $\varkappa$)

$$= 2\pi\varepsilon n^5 \sin\phi \; \underline{J}'_{\varkappa}(\varkappa)$$ — derivative of Anger function

$$\underline{J}'_{\varkappa}(\varkappa) = \frac{1}{2\pi}\int_{-\pi}^{\pi} \sin(\varkappa(\xi-\sin\xi))\sin\xi \, d\xi$$

For integer $\varkappa \to \underline{J}'_{\varkappa}(\varkappa) = J'_{\varkappa}(\varkappa) \approx \frac{0.411}{\varkappa^{2/3}}$

$$\Delta N = \frac{\Delta n}{\omega n^3} = \frac{\Delta E}{\omega}; \qquad k = 2\pi \cdot 0.411\,\varepsilon/\omega^{5/3} = \frac{2.6\varepsilon}{\omega^{5/3}}$$

(F22)

$$\Delta N = \frac{2\pi\varepsilon n^2}{\omega}\sin\phi \; \underline{J}'_{\varkappa}(\varkappa) = k A(\varkappa)\sin\phi$$

$$A(\varkappa) = \varkappa^{2/3}\,\underline{J}'_{\varkappa}(\varkappa)/0.411 \to 1 \quad (\varkappa \gg 1)$$

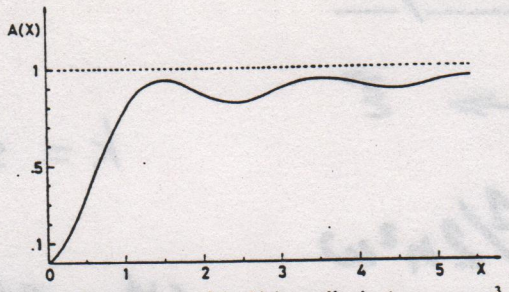

Fig. 1. Dependence of the kick amplitude $A$ on $\chi = \omega n^3$.

corresponding to the change in $n$ given by (11) is

$$\Delta N = \Delta n/(n^3\omega) = (2\pi\epsilon n^2/\omega)\, J'_\chi(\chi) \sin\phi. \quad (12)$$

For integer values of $\chi$, the Anger functions coincide with ordinary Bessel functions, and for $\chi \to \infty$ they have the same asymptotic behavior. That is, on defining

$$A(\chi) = (\chi^{2/3}/0.411) J'_\chi(\chi),$$

we have $A(\chi) \approx 1$ for $\chi >> 1$. (See the above given asymptotics of $J'_s(s)$.) Instead, for $\chi \to 0$, $J'_\chi(\chi) \sim \chi/2$; the behavior of $A(\chi)$ is illustrated in Fig. 1. We can rewrite (12) as

$$\Delta N = kA(\chi) \sin\phi \qquad k = 0.822\pi\epsilon\omega^{-5/3}. \quad (13)$$

A stationary-phase analysis of (11) shows that for large $\chi$, the main change in action occurs within a small interval $\Delta\xi \sim \chi^{-1/3} << 1$ near the stationary phase point $\xi = 0$. Therefore, as we anticipated above, for large $\chi$ the monochromatic perturbation is mainly effective when the electron is very close to the perihelion.

Now we shall regard $N$, $\phi$ as a pair of canonically conjugate variables and seek for a canonical map connecting the values of $N$, $\phi$ at consecutive passages at the aphelion. The above developed perturbation theory yields (13) for the change in $N$ at first order and $\Delta\phi = 2\pi\omega(-2\omega\bar{N})^{-3/2}$ for the change in $\phi$ at zero order. Following a standard procedure [35], we can now look for a generating function $G(\bar{N}, \phi)$ such that the map defined by

$$N = \partial G/\partial\phi \qquad \bar{\phi} = \partial G/\partial\bar{N}$$

coincides at first order and zero order, respectively, with our perturbative result.

This function is

$$G(\bar{N}, \phi) = \bar{N}\phi + 2\pi(-2\omega\bar{N})^{-1/2} + kA(\bar{\chi}) \cos\phi \quad (14)$$

with $\bar{\chi} = \omega(-2\omega\bar{N})^{-3/2}$. It generates the following map

$$\bar{N} = N + kA(\bar{\chi}) \sin\phi$$
$$\bar{\phi} = \phi + 2\pi\omega(-2\omega\bar{N})^{-3/2} + 3k\omega^2(-2\omega\bar{N})^{-5/2} A'(\bar{\chi}) \cos\phi. \quad (15)$$

Notice that the implicit character of (15) cannot be avoided if a canonical (area preserving) map is required. For the same reason, the second equation (15) contains a first-order correction to the above perturbative result for $\Delta N$, $\Delta\phi$.

Since $A(\chi) \sim 1$ for $\chi >> 1$, the map (15) is greatly simplified in the region of large $\chi$, i.e., of large $\omega_0$- where it takes the form of the following "Kepler map:"

$$\bar{N} = N + k \sin\phi$$
$$\bar{\phi} = \phi + 2\pi\omega(-2\omega\bar{N})^{-3/2}. \quad (16)$$

On the other hand as can be seen from Fig. 1, $A(\chi)$ is already close to 1 for $\chi = 1$; therefore, the map (16) provides an acceptable description of the motion for $\omega_0 \gtrsim 1$. Notice that even though the map (16) is canonical, hence area preserving, it is not defined on all bound states ($N < 0$); indeed, it carries some bound states into the positive energy region, where $\phi$ is no longer defined. When this happens, the electron escapes to infinity and ionization occurs.

The effect of a small static field $\epsilon_s$ superimposed to the monochromatic field would essentially be a change in the Kepler period. Then for small $\epsilon_s$ only the second equation (16) should be modified by adding a term

$$-6\pi\omega\epsilon_s(-2\omega\bar{N})^{-7/2}.$$

We obtained a numerical check of the validity of the mapping (16) as an approximate description of the dynamics, by the following procedure. By numerically solving the exact equations of motion (10), we computed the sequence $\phi_j = \omega t_j$ of the phases at passages of the electron at the perihelion. Next, by computing $N_j = (-2\omega)^{-1}[(\phi_j - \phi_{j-1})/2\pi\omega)]^{-2/3}$ we found $g(\phi_j) = k^{-1}[N_j - N_{j+1}]$ and we plotted this against $\phi_j$ for several values of $k$. The comparison of the result to the theoretical prediction $k^{-1}[N_{j+1} - N_j] = \sin\phi_j$ is given in Fig. 2; even for $\omega_0 = 1.5$, the agreement between numerical and theoretical data is very good.

## IV. Diffusive Excitation and Ionization in the 1-D Classical Model

The mapping (16) allows for a straightforward estimate of the critical field value required for the transition to chaotic motion. By linearizing the second equation (16), we obtain the map

$$\bar{N} = N + k \sin\phi$$
$$\bar{\phi} = \phi + T\bar{N} \quad (17)$$

where $T = 6\pi\omega^2 n_0^5$ (an unessential constant has been dropped in the second equation). Equation (17) is the celebrated standard map. As is well known, the onset of stochasticity for this map occurs when the stochasticity parameter $K = kT$ becomes larger than 1.

Then, defining $\epsilon_c$ by $K = \epsilon_0/\epsilon_c$, we obtain the condition for unlimited chaotic excitation in the form $\epsilon_0 > \epsilon_c$, with $\epsilon_c$ given by

$$\epsilon_c \approx 1/(49\omega_0^{1/3}). \quad (18)$$

This estimate follows from the simplified map (17) which is a good approximation to the true dynamics when $\omega_0 >$

# Kepler map



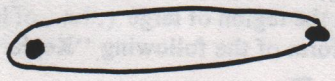

$\vec{\varepsilon}$

$$k = \frac{2.6\,\varepsilon}{\omega^{5/3}}$$

$$N = E/\omega = -\,1/2n^2\omega$$

$\omega t$ at perihelion

(F23) (a,b,c)

$$\begin{cases} \bar{N} = N + k\sin\phi \\ \bar{\phi} = \phi + 2\pi\omega\left[-2\omega\bar{N}\right]^{-3/2} \end{cases}$$

after one orbital period

$$2\pi\omega n^3$$

$$l < \left(\frac{3}{\omega}\right)^{1/3}$$

$$\omega_0 = \omega n^3 > 1$$

Local description by Chirikov standard map (linearization of second equation

$$\bar{N} = N + k\sin\phi \;;\; \bar{\phi} = \phi + T\bar{N}$$

$$T = \frac{\partial(\Delta\phi)}{\partial N} = 2\pi\omega\cdot 3n^2\cdot\frac{dn}{dE}\omega = 6\pi\omega^2 n^5$$

Global chaos:

$$K = kT = 6\pi\cdot 2.6\,\frac{\varepsilon}{\omega^{5/3}}\cdot\omega^2 n^5 = 49\,\varepsilon_0\,\omega_0^{1/3} > 1$$

$$\longrightarrow \quad \varepsilon_0 = \varepsilon n_0^4 > \frac{1}{49\,\omega_0^{1/3}} \;;\; \omega_0 = \omega n_0^3 > 1$$

Diffusion rate (in number of orbital periods)

$$D = \frac{(\Delta N)^2}{\Delta t} = \frac{k^2}{2} \approx 3.33\,\frac{\varepsilon^2}{\omega^{10/3}} = 3.33\,\frac{\varepsilon_0^2 n_0^2}{\omega_0^{10/3}}$$

Ionization time

$$t_I \approx \frac{N_I^2}{D} \approx \frac{\omega_0^{4/3}}{13\,\varepsilon_0^2} \gg 1 \qquad N_I = \frac{n_0}{2\omega_0} = \frac{1}{2n^2\omega}$$

Casati, Guarneri, Shepelyansky



Kepler map

$$\bar{N} = N + k g(\phi)$$
$$\bar{\phi} = \phi + 2\pi\omega(-2\omega\bar{N})^{-\frac{3}{2}}$$

$$E_0 = \omega N \cdot n_0^2$$
$$k = \frac{2.6\,\varepsilon}{\omega^{5/3}}$$
$$g = \sin\phi$$

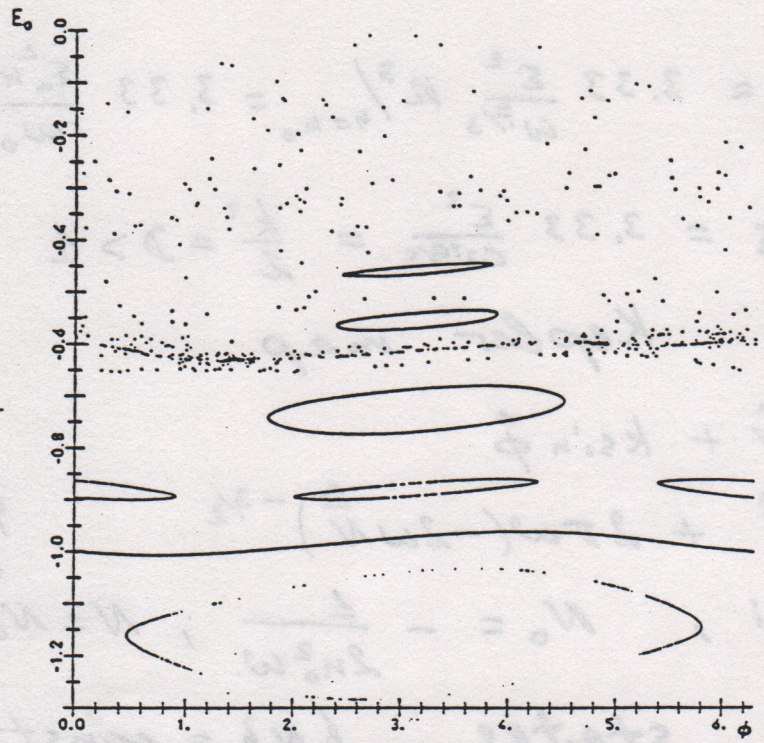


Fig. 3. Phase space portrait for the map (16) in the variables $E_0 = \omega N n_0^2$ $= -n_0^2/2n^2$, $\phi$. Parameter values are $\epsilon_0 = 0.03$, $\omega_0 = 3.5$. Six regular and one chaotic trajectory are shown.



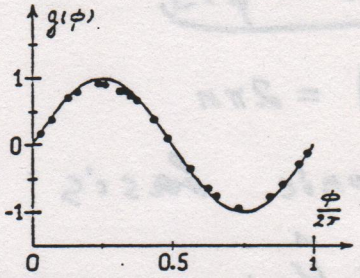


Fig. 2. Numerically computed function $g(\phi_j)$ (dots) compared to the theoretical curve sin $\phi$ (full curve) for the case $\epsilon_0 = \epsilon n_0^4 = 0.04$, $\omega_0 = \omega n_0^3 = 1.5$

(42)

# Photonic localization

(F24)

$$l_s \approx D|_{n=n_0} \approx 3.33\,\frac{\varepsilon^2}{\omega^{7/3}}\,n^3|_{n=n_0} = 3.33\,\frac{\varepsilon_0^2 n_0^2}{\omega_0^{7/3}}$$

$$l_\phi = \frac{l_s}{\omega n^3} = 3.33\,\frac{\varepsilon^2}{\omega^{10/3}} = \frac{k^2}{2} = D > 1 \quad \left(\begin{matrix} k \gtrsim 1 \\ \text{Shuryak} \\ \text{border}\end{matrix}\right)$$

Quantum Kepler map

$$\begin{cases} \hat{\bar{N}} = \hat{N} + k\sin\hat{\phi} \\ \hat{\bar{\phi}} = \hat{\phi} + 2\pi\omega(-2\omega\hat{\bar{N}})^{-3/2} \end{cases}$$

quasimomentum

$$[\hat{N}, \hat{\phi}] = -i\,, \quad N_0 = -\frac{1}{2n_0^2\omega}\,; \quad N = N_0 + N_\phi$$

**Photonic states** $\{N\} = \text{const}$

$$\hat{N}_\phi = -i\frac{\partial}{\partial\phi}\,; \quad 0 \le \phi \le 2\pi\,;$$

$$H = \underbrace{2\pi[-2\omega\,(N_0 + \hat{N}_\phi)]^{-1/2}}_{H_0(N_\phi) = 2\pi n} + k\cos\phi\,\delta_1(t)$$

Kepler Map in photonic basis:

$$\bar{\Psi} = \underset{\text{ionization}}{P}\,\exp(-i\frac{\hat{H}_0}{2})\exp(-ik\cos\phi)\exp(-i\frac{\hat{H}_0}{2})\,\Psi$$

(projection on discrete states)

(F25)

$$\Psi_N \propto \exp(-2|N - N_0|/l_\phi)$$

(F26)

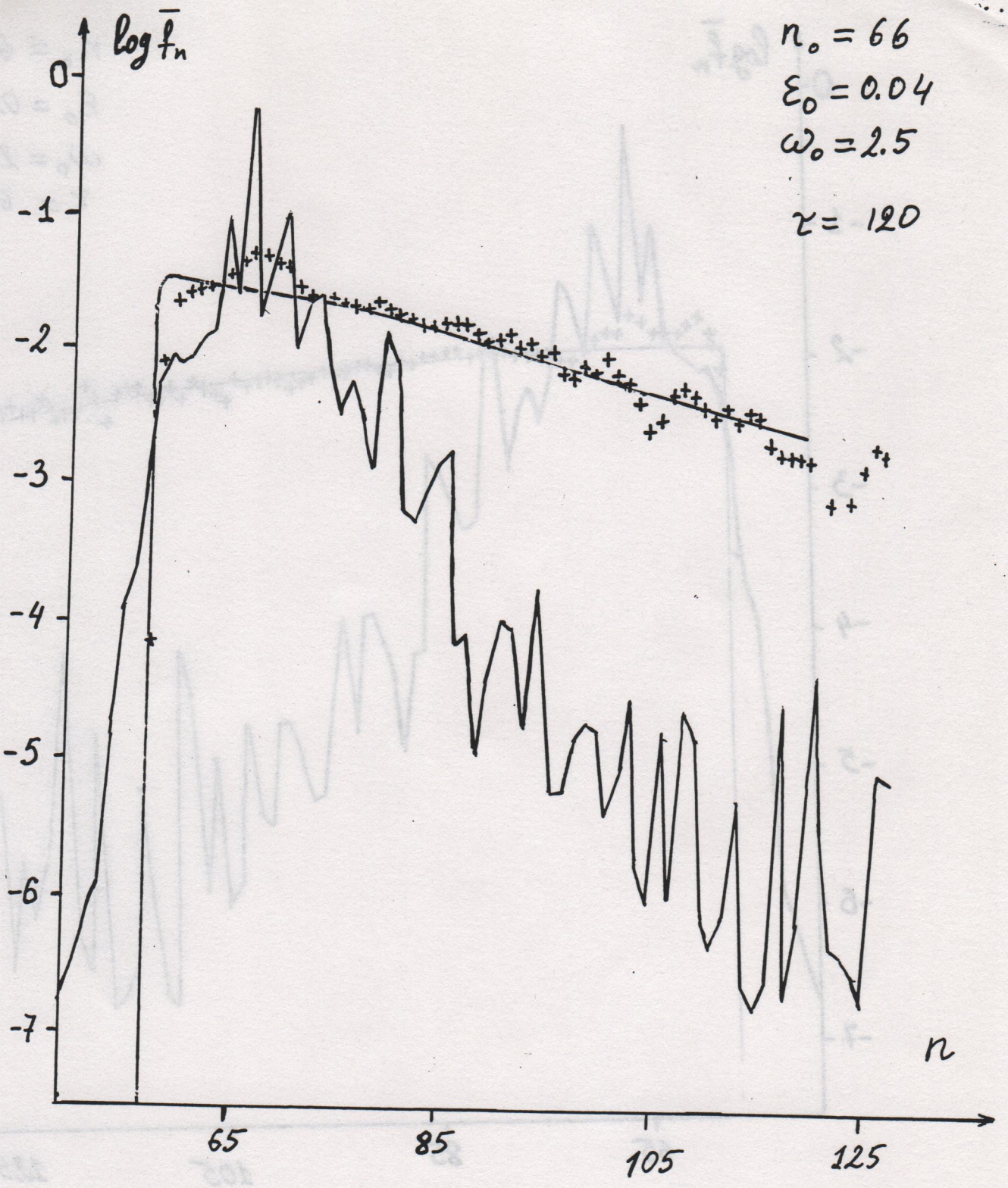
$\log \bar{f}_n$
0
-1
-2
-3
-4
-5
-6
-7
$n_0 = 66$
$\varepsilon_0 = 0.04$
$\omega_0 = 2.5$
$\tau = 120$
n
65
85
105
125

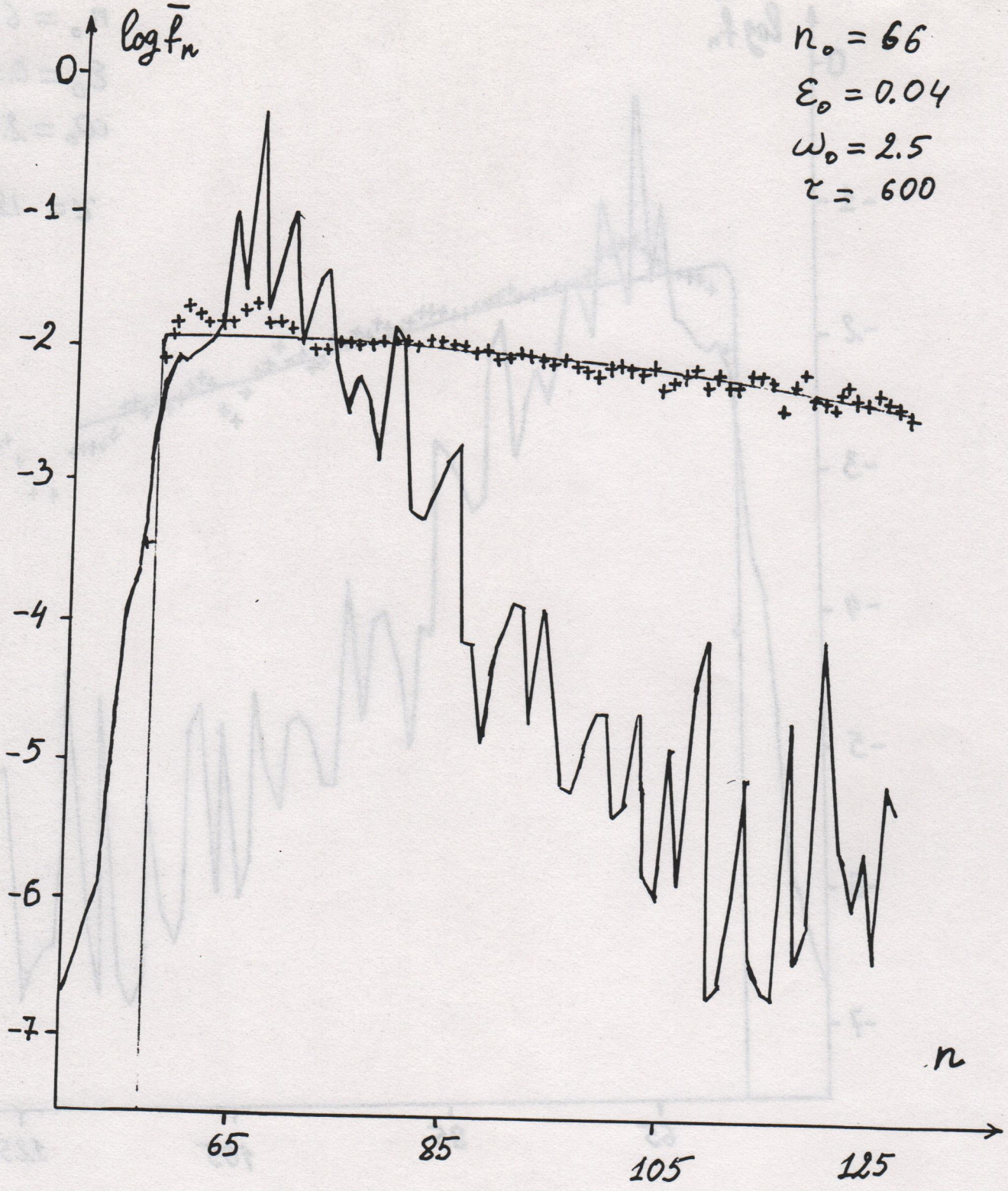
$\log \bar{f}_n$
0
-1
-2
-3
-4
-5
-6
-7
$n_0 = 66$
$\varepsilon_0 = 0.04$
$\omega_0 = 2.5$
$\tau = 600$
n
65
85
105
125

Casati, Guarneri, Shepelyansky (1987)

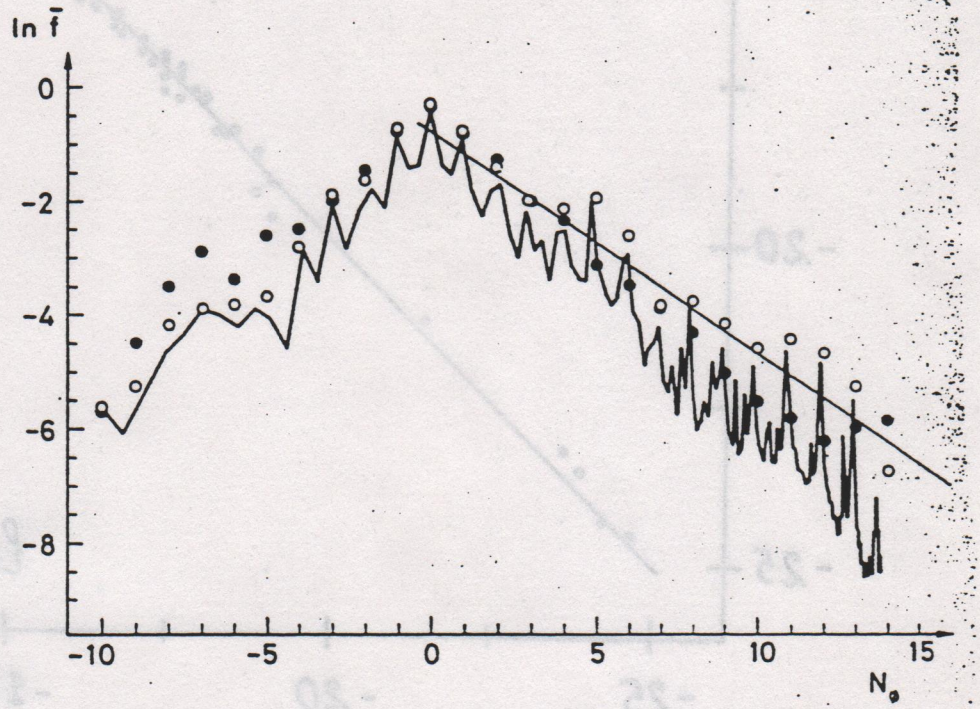


FIG. 1. The probability distribution, averaged from 80 to 120 periods vs the number of photons $N_\phi = N_I - 1/(2n^2\omega)$. Here $n_0 = 100$, $\varepsilon_0 = \varepsilon n_0^4 = 0.04$, $\omega_0 = \omega n_0^3 = 3$. For each integer value of $N_\phi$, open circles indicate the probability in the interval $N_\phi - \frac{1}{2}$, $N_\phi + \frac{1}{2}$. The straight line is the result of a least-squares fitting of the peak's value. Filled circles were obtained by iterating the quantum map (6) (quantum Kepler map).

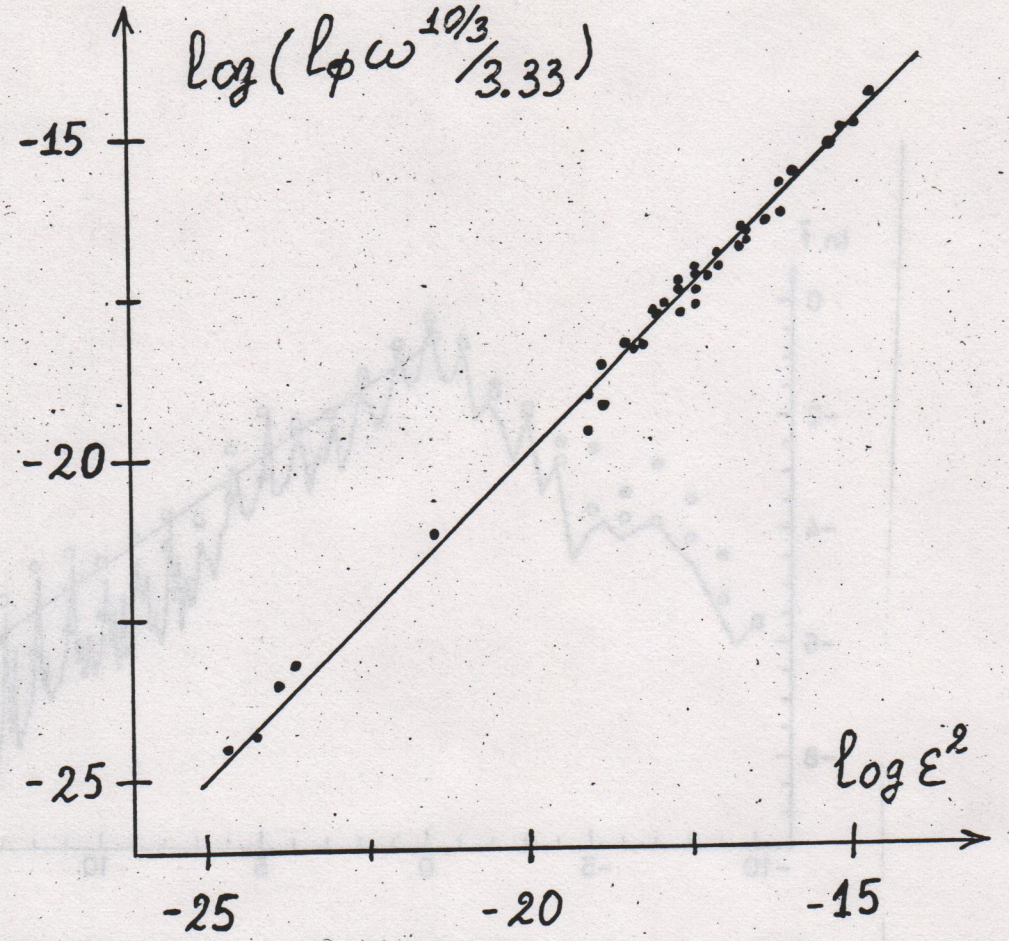


43 distributions with $l_{\varphi\,teor} > 1$

$30 \le n_o \le 500, \quad 1 \le \omega_o \le 3.5$

# A Model of Molecular Excitation

(Akulin, Dykhne 197)

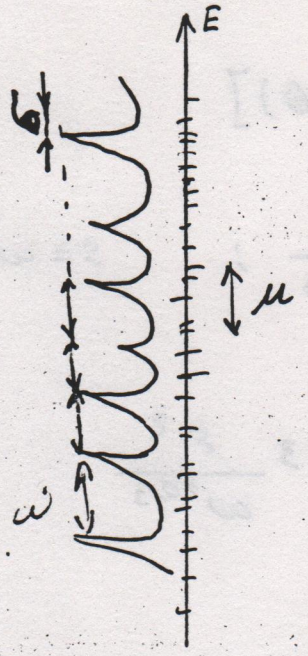


$\rho$, $\mu$, $\omega\rho \gg 1$

Fermi golden rulle

$$W = \frac{\pi}{2} |\mu(E, E+\omega)|^2 \varepsilon^2 \rho$$

Diffusion rate in energy

$$D_E = \frac{(\Delta E)^2}{\Delta \tau} = 2W\omega^2 \frac{2\pi}{\omega} = 2\pi^2 \mu^2 \varepsilon^2 \rho \omega$$

$\tau$ - time in number of periods

$$D_n = \frac{(\Delta n)^2}{\Delta \tau} = \rho^2 D_E$$

$$l_s = D_n = 2\pi^2 \mu^2 \varepsilon^2 \omega \,, \quad l_{sE} = l_s/\rho$$

$$\boxed{l_\varphi = \frac{l_s}{\omega\rho} = 2\pi^2 \mu^2 \varepsilon^2 \rho^2 = 2\pi D_\varphi \rho} \quad \boxed{\sim \Gamma\rho}$$

with $D_\varphi = \pi \mu^2 \varepsilon^2 \rho$ - diffusion rate in number of photon per unit of time

$\Gamma \sim \delta \sim \mu^2 \varepsilon^2 \rho \lessgtr \omega$ ; $\Gamma \sim D_\varphi$

Number of excited states:

$$N \sim (D_\varphi t)^{1/2} \,, \quad \delta n \sim N\rho\delta \sim (D_\varphi t)^{1/2} \rho \delta$$

$$\Delta V \sim \frac{\delta}{\delta n} \sim \frac{1}{N\rho}$$ peak width (independent on $\delta$)

$$t^* \sim \frac{1}{\Delta V} \sim N\rho \sim \rho (D_\varphi t^*)^{1/2} \sim \rho^2 D_\varphi$$

$$l_\varphi \sim N(t^*) \sim D_\varphi \rho \sim \mu^2 \varepsilon^2 \rho^2$$

(44) For hydrogen

$$H = -\frac{1}{2n^2} + n^2\varepsilon\cos\omega t\left[\frac{3}{2} - 2\sum_{s=1}^{\infty} x_s \cos(s\theta)\right]$$

$$\mu = n^2 x_s \simeq n^2 \frac{0.411}{s^{5/3}} \approx \frac{0.411}{n^3\omega^{5/3}}; \qquad s = \omega n^3$$

$$\rho = n^3$$

$$l_\varphi = 2\pi^2 (0.411)^2 \frac{\varepsilon^2}{\omega^{10/3}} = 3.33\frac{\varepsilon^2}{\omega^{10/3}}$$

## Delocalization

$$l_\varphi = 3.33\frac{\varepsilon_0^2 n_0^2}{\omega_0^{10/3}} = \frac{k^2}{2} > N_I = \frac{n_0}{2\omega_0}$$

$$\varepsilon_0 > \varepsilon_q = \frac{\omega_0^{7/6}}{\sqrt{6.6 n_0}} = \frac{\omega^{1/6}}{\sqrt{6.6}}\omega_0 \qquad (\omega = \text{const})$$

$\rightarrow$ 0.042 for 10GHz

Cut off in experiment at $n_c$

$$N_I \rightarrow N_c = \frac{1}{2\omega}\left(\frac{1}{n_0^2} - \frac{1}{n_c^2}\right) = \frac{n_0}{2\omega_0}\left(1 - \frac{n_0^2}{n_c^2}\right)$$

$$\varepsilon_q \rightarrow \varepsilon_q = \frac{\omega^{1/6}}{\sqrt{6.6}}\omega_0\left(1 - \frac{n_0^2}{n_c^2}\right)^{1/2}$$

10% border $\rightarrow$ steady-state distribution

$$\bar{f}(N) = \frac{1}{2l_\varphi}\left(1 + \frac{2|N|}{l_\varphi}\right)\exp\left(-\frac{2|N|}{l_\varphi}\right)$$ as in kicked rotator

$$W_I = 0.1 = \int_{N_c}^{\infty} \bar{f}(N)\,dN \rightarrow \frac{1}{\sqrt{6.6}} \rightarrow \frac{1}{\sqrt{8}}$$

(=27,28,29)

$\varepsilon n_0^7$ Koch et al. 1983

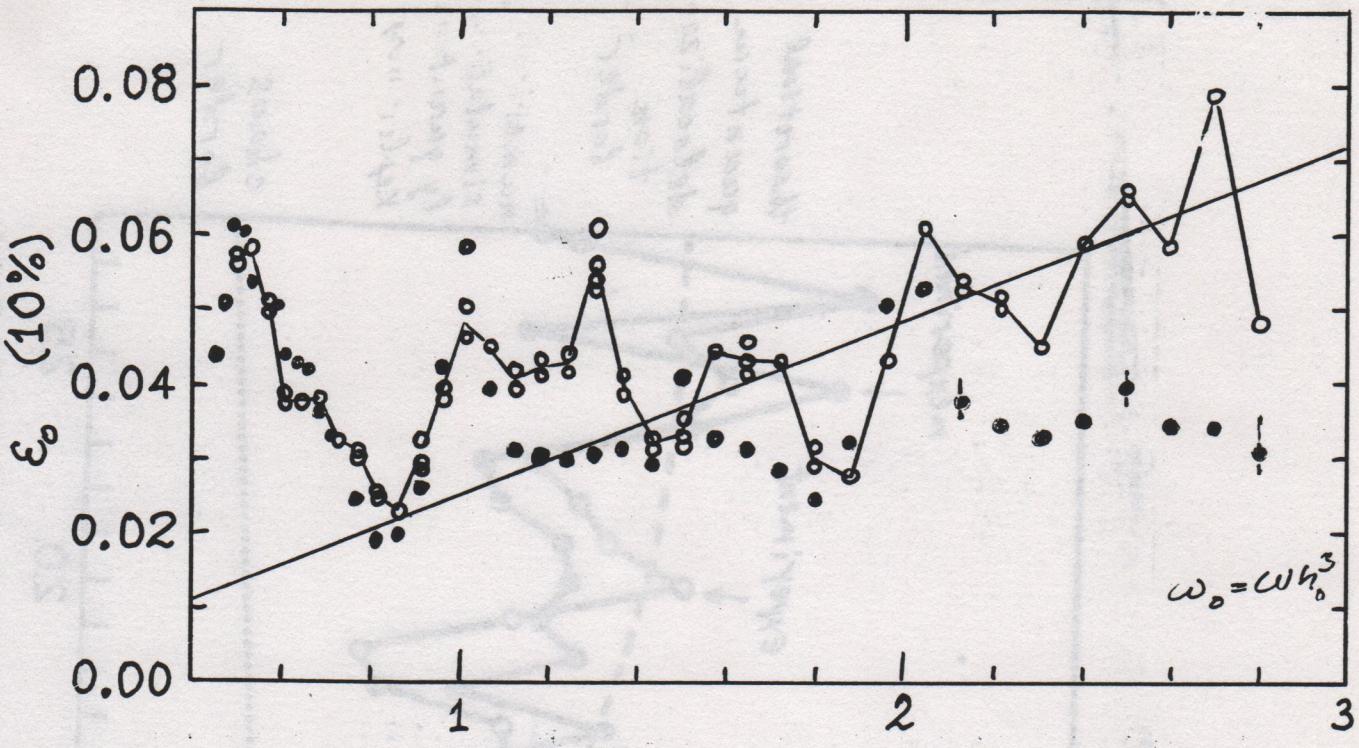


$\omega_0=\omega n_0^3$ $(\omega/2\pi = 36.02$ GHz)

$n_0 = 45 \div 80$

o - experimental data

• - classical numerical data

—— - delocalization border with the experimental value of $n_0$



(127)

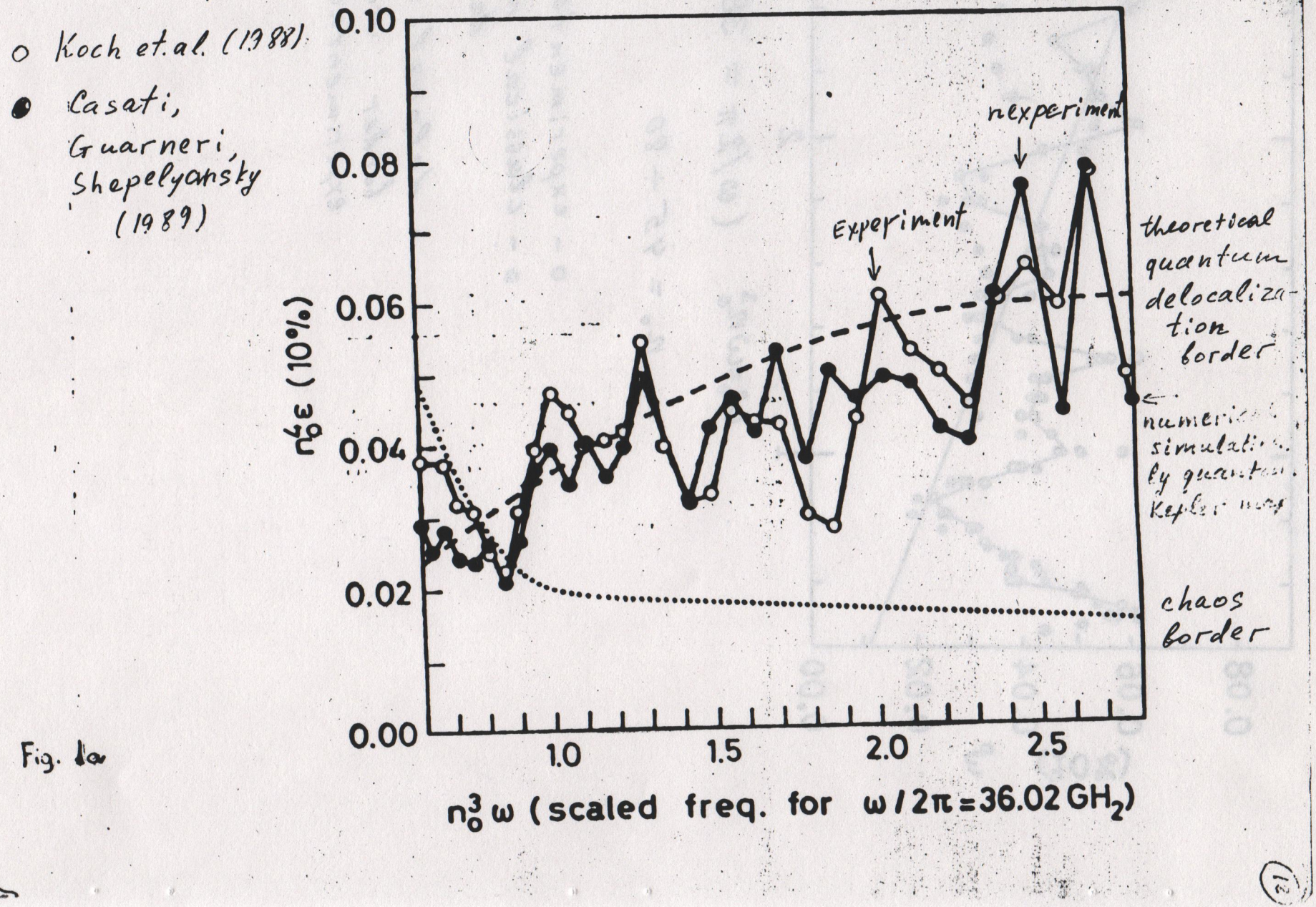
o Koch et.al. (1988)
● Casati, Guarneri, Shepelyansky (1989)
0.10
0.08
0.06
0.04
0.02
0.00
$n^4\varepsilon$ (10%)
1.0
1.5
2.0
2.5
$n_0^3\omega$ (scaled freq. for $\omega/2\pi = 36.02\,GH_2$)
experiment
Experiment
theoretical quantum delocalization border
numerical simulation by quantum Kepler map
chaos border

Fig. 1a

Bayfield et al. (1989)

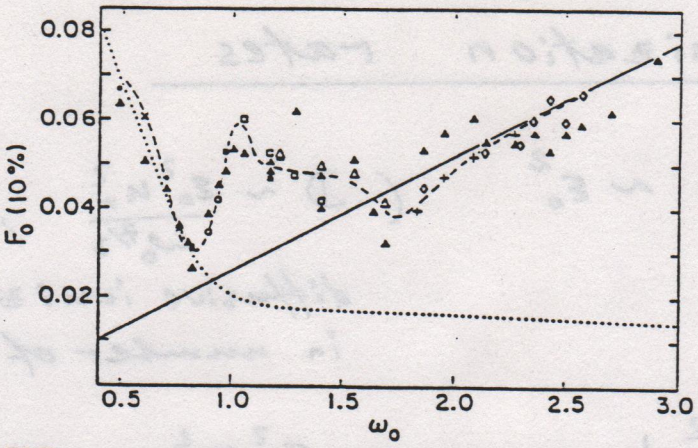


▲ - 1d Shroedinger equation numerical simulations

FIG. 1. A comparison at identical parameter values of experimental and quantum-mechanical values for the microwave field strength for 10% ionization probability, as a function of microwave frequency. The field and frequency are classically scaled, $\omega_0 = n_0^3\omega$ and $F_0 = n_0^4 F$. Ionization includes excitation to states with $n$ above $\bar{n}$. The theoretical points are shown as solid triangles. The dashed curve is one drawn through the entire experimental data set shown in Fig. 2. Values of $n_0$, $\bar{n}$ are ●, 64, 114; ×, 68, 114; ○, 71, 114; ■, 76, 114; □, 80, 120; △, 86, 130; +, 94, 130; ◇, 98, 130. Multiple theoretical values at the same $\omega_0$ are for different compensating experimental choices of $n_0$ and $\omega$. The dotted curve is the classical chaos border. The solid line is the quantum 10% threshold according to localization theory for the present experimental conditions.

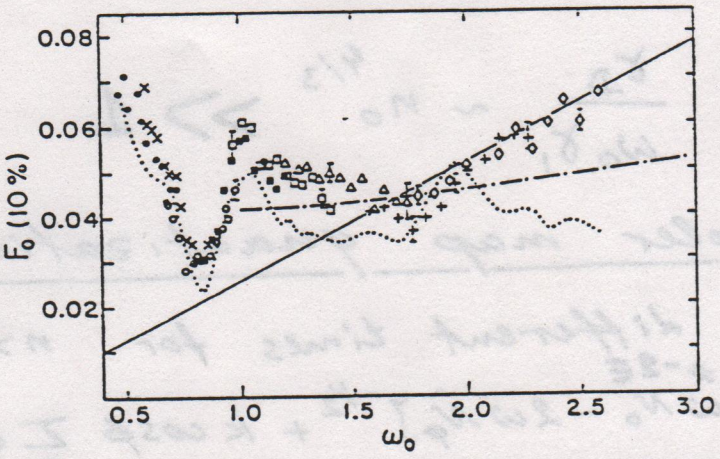


FIG. 2. Experimental data as in Fig. 1, compared with the results of one-dimensional model classical calculations (dotted line) and with one-dimensional model predictions for quantum suppression by cantori in phase space (dash-dotted curve). The solid line of Fig. 1 is also included. The dotted line was created by drawing through every point obtained for the parameter values used for the solid triangles of Fig. 1.

# Ionization rates

$$\gamma_D \sim \frac{D}{n_0^2} \sim \varepsilon_0^2 \qquad \left( D \sim \frac{\varepsilon_0^2 n_0^2}{\omega_0^{7/3}},\ \omega_0 \sim 1 \right)$$

diffusive ionization rate in number of microwave period

$$\gamma_1 = \left(\frac{k}{2}\right)^2 \frac{1}{\omega_0} = 1.67\, \frac{\varepsilon_0^2 n_0^2}{\omega_0^{10/3}\omega_0} \sim \frac{\varepsilon_0^2}{n_0^{7/3}} \quad (\omega_0 = \frac{n_0}{2},$$

one-photon ionization rate in number of microwave peri

$$\frac{\gamma_D}{\gamma_1} \sim n_0^{7/3}$$

Real widthes in physical time:

(F21)
$$\frac{\Gamma_D}{\Gamma_1} \sim \frac{\gamma_D}{\omega_0 \gamma_1} \sim n_0^{4/3} \gg 1$$

## Kepler map quantization

Problem of different times for $n \gg n_0$

$$H = 2\pi \left[ \overbrace{-2\omega N_0}^{=-2E} - 2\omega \hat{N}_\phi \right]^{-1/2} + k\cos\phi \sum_m \delta_1(t-m)$$

One-orbital period map:

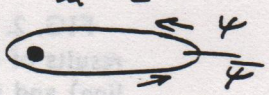


$$\Psi = \left[ \exp\left(-i\pi \left[-2E - 2\omega \hat{N}_\phi\right]^{-1/2}\right) \exp(-ik\cos\phi) \cdot \right.$$
$$\left. \cdot \exp\left(-i\pi \left[-2E - 2\omega \hat{N}_\phi\right]^{-1/2}\right) \right] \Psi = U_- \Psi = \Psi$$

$\Psi = U_- \Psi = \Psi \rightarrow E = E_n - i\Gamma_n/2 \quad (k=0 \rightarrow E_n = -\frac{1}{2n^2})$

scattering problem: $U = \exp(i\delta_N)\exp(-ik\cos\phi)\exp(i\delta_N)$

$U = \begin{pmatrix} U_+ & iR_+ \\ -iR_- & U_- \end{pmatrix}$; S-matrix: $S = U_+ + R_+(1+U_- + U_-^2 \ldots)R_- = U_+ + R_+ \frac{1}{1-U_-} R_-$

(46)

# Localization in 2D-Hydrogen

$$\Delta n = -\int_0^{2\pi n^3} dt\,\frac{\partial H}{\partial \theta}\,, \qquad \Delta l = -\int_0^{2\pi n^3} dt\,\frac{\partial H}{\partial \psi}$$

$$\Delta\phi \approx -2\pi n^3\omega\,, \qquad \Delta\psi = \int_0^{2\pi n^3} dt\,\frac{\partial H}{\partial l}\,; \qquad \phi = s\theta - \omega t$$

Generating function: $G(\bar N, \bar l, \phi, \psi)$

New variables:

| | |
|---|---|
| slow | $N, l, \psi$ |
| Fast | $\phi$ |

$$\tan\chi = \left(\frac{B}{A}\right)\tan\psi\,, \qquad \Phi = \phi + \chi$$

$$J + N = \int_0^l dl'\, AB/(A^2\sin^2\chi + B^2\cos^2\chi)$$

$$A = 1 - Nl^2\omega\,; \qquad B = 1.09\,\omega^{1/3} l$$

$$(N, \Phi; J, \chi)\,; \quad \mathcal{H}^2(N, J, \chi) = A^2\cos^2\psi + B^2\sin^2\psi$$

$$\bar N = N - k\mathcal{H}\sin\Phi$$

$$\bar\Phi = \Phi - 2\pi\omega(-2\omega\bar N)^{-3/2} - k\left(\frac{\partial\mathcal{H}}{\partial\bar N}\right)\cos\bar\Phi$$

$$\bar J = J + k\cos\bar\Phi\cdot\frac{\partial\mathcal{H}}{\partial\chi}$$

$$\bar\chi = \chi - k\cos\bar\Phi\,\frac{\partial\mathcal{H}}{\partial\bar J}$$

New <u>chaotic</u> time $\sigma$: $d\sigma/dt = k\cos\bar\Phi$

Weak dependence of $\mathcal{H}$ on $\bar N$: $(J,\chi) \to (l,\psi)$

$$\mathcal{H} = [(1 + l^2/2n^2)^2\cos^2\psi + (1.09\,\omega^{1/3} l)^2\sin^2\psi]^{1/2}$$ integral of motion

$$\frac{\partial l}{\partial\sigma} = \frac{\partial\mathcal{H}}{\partial\psi}\,; \qquad \frac{\partial\psi}{\partial\sigma} = -\frac{\partial\mathcal{H}}{\partial l}\,;$$

$$\mu_1 = \langle n_2 - n_{20}\rangle$$

$$\mu_2 = \langle (n_2 - \langle n_2\rangle)^2\rangle$$

(F-30) (F-31) (F-32) for $2\sigma \ll n \to \mu_2/(\mu_1 n_{20}) \approx 1$

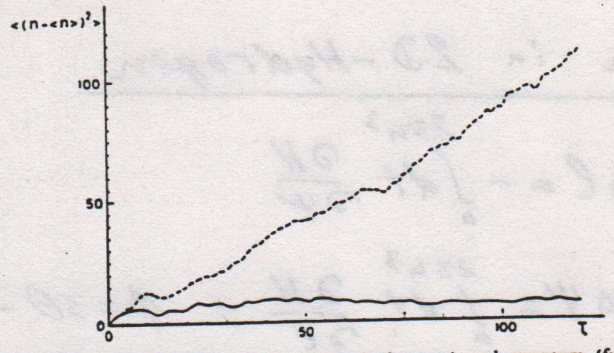


Fig. 8. Dependence of the classical (dashed curve) and quantum (full curve) second moments of the distribution $f(n)$ on the number of microwave periods $\tau$. Parameter values are $n_0 = 66$, $\omega_0 = 2.5$, $\epsilon_0 = 0.04$, and $n_{20} = 15$. The straight, dotted line gives the theoretical estimate for the classical diffusion rate (see the text).

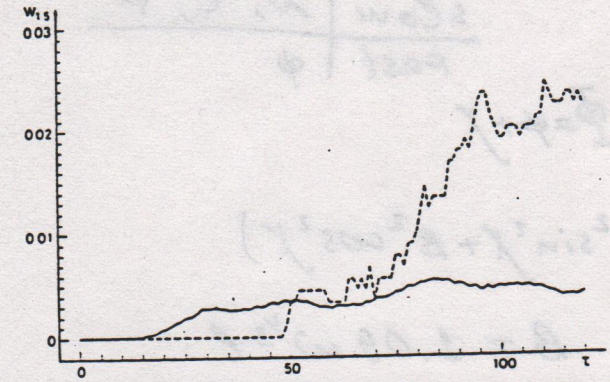


Fig. 9. Classical (dashed curve) and quantum (full curve) excitation probability $W_{1.5}$ above the level $n = 1.5\,n_0$ as a function of the number $\tau$ of microwave periods for the same parameter values of Fig. 8. In the figure, the quantum probability is multiplied by a factor 100.



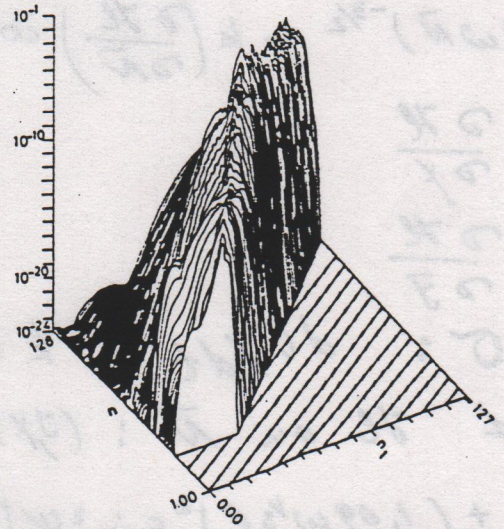


Fig. 12. An example of a full quantum probability distribution $F(n, n_1)$ for the same case of Fig. 10.

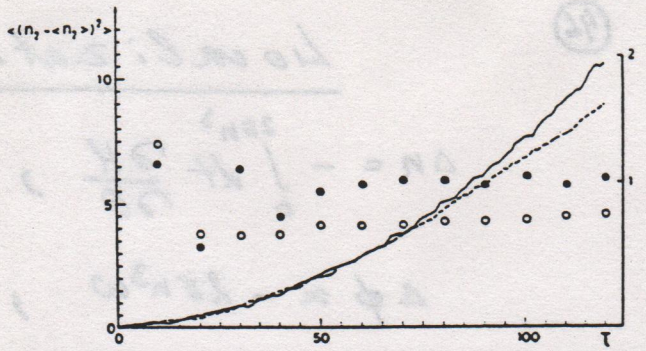


Fig. 11. Time dependence of second moments $\mu_2$ of $n_2$ for the classical (dashed line) and quantum (full curve) distributions for the same parameter values of Fig. 10. Here we also show the ratio of $n_2/n_{20}$ to the first moment $\mu_1$ of $n_2$ in the classical case (open circles) and in the quantum case (full circles). It is seen that this ratio is close to one (right-hand scale) in agreement with the theoretical expression (51).

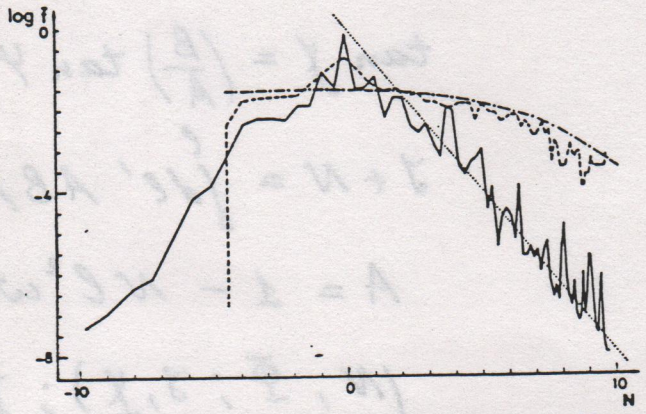


Fig. 10. Classical (dashed curve) and quantum (full curve) distribution functions, averaged in the time interval $110 < \tau \leq 120$, versus the number of absorbed photons $N = (1/2n_0^2 - 1/2n^2)/\omega$ for the same parameter values of Fig. 9. The straight, dotted line is the one-dimensional, quantum, theoretical exponential distribution; the dotted-dashed curve is the analytical solution of the Fokker–Planck equation.

Casati, Guarneri, Shepelyansky (1988)

F30

Casati, Chirikov, Guarneri, Shepelyansky (1986)

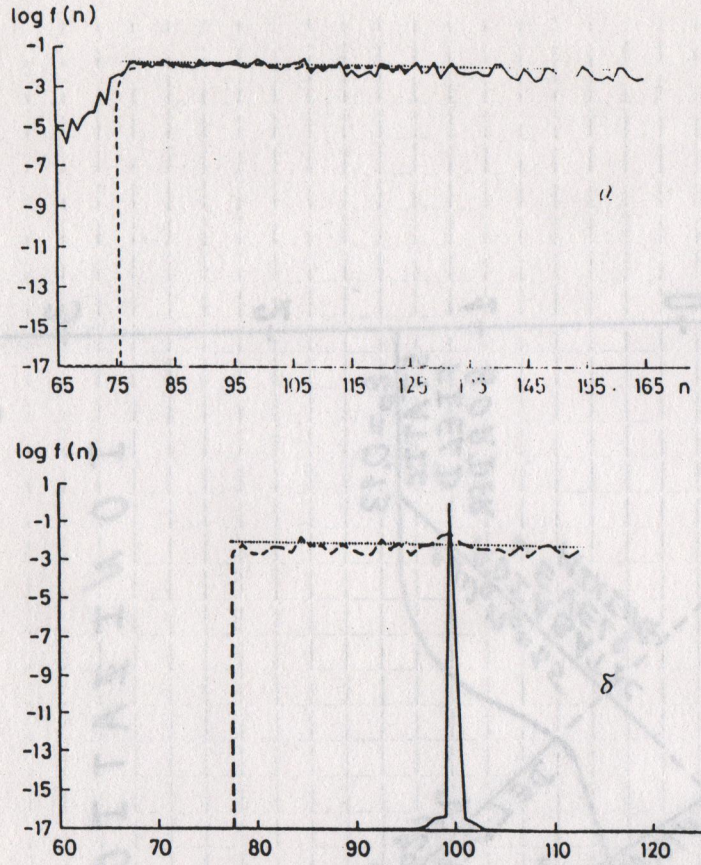


*Рис. 23.* *а* — Классическое (штриховая линия) и квантовое (сплошная линия) распределения $f(n)$ для $n_0 = 100$, $\varepsilon_0 = 0.08$, $\omega_0 = 1.5$ в момент времени $\tau = 60$. Пунктирная линия — аналитическое решение (3.2.8) уравнения ФПК. *б* — Эти же распределения в момент времени $\tau = 120$ после обращения скоростей (времени) при $\tau = 60$. Классическое распределение удовлетворительно согласуется с (3.2.8) при $\tau = 120$.



τ = 60

τ = 120

Time reversability

God does not play dice.
A. Einstein

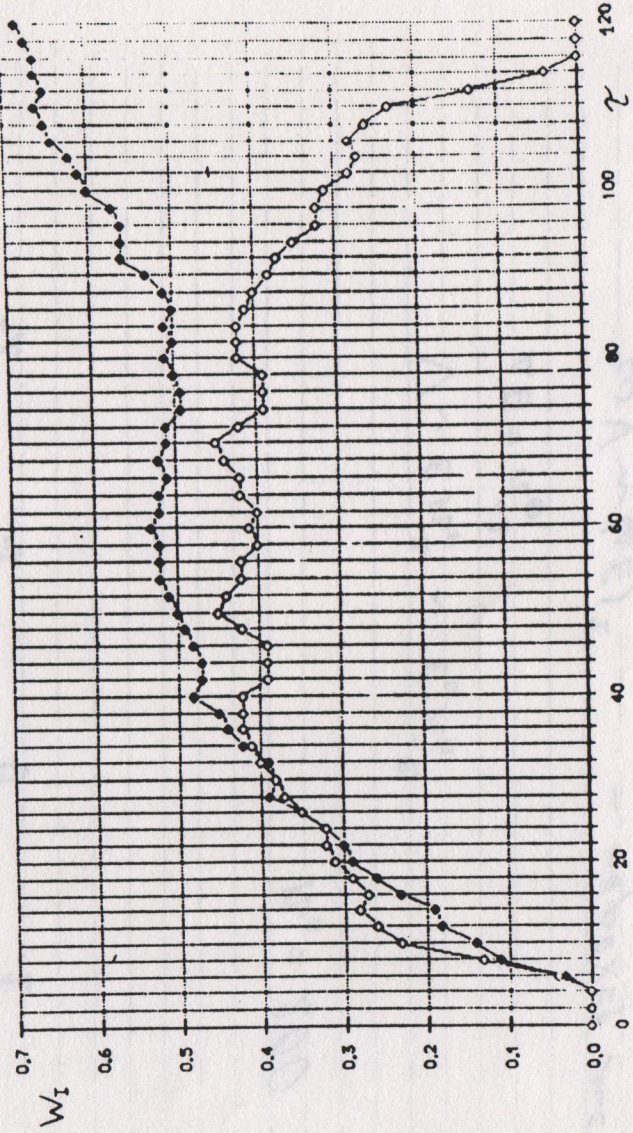


*Рис. 24.* Классическая (◆) и квантовая (○) вероятности ионизации $W_I$ [illegible] $n_0 = 100$, $\varepsilon_0 = 0.08$, $\omega_0 = 1.5$ [illegible]

$n_0 = 100$, $\varepsilon_0 = 0,08$, $\omega_0 = 1,5$ — Ionization probability $W_I$

◆ - classical, ○ - quantum

(95)

(F31)

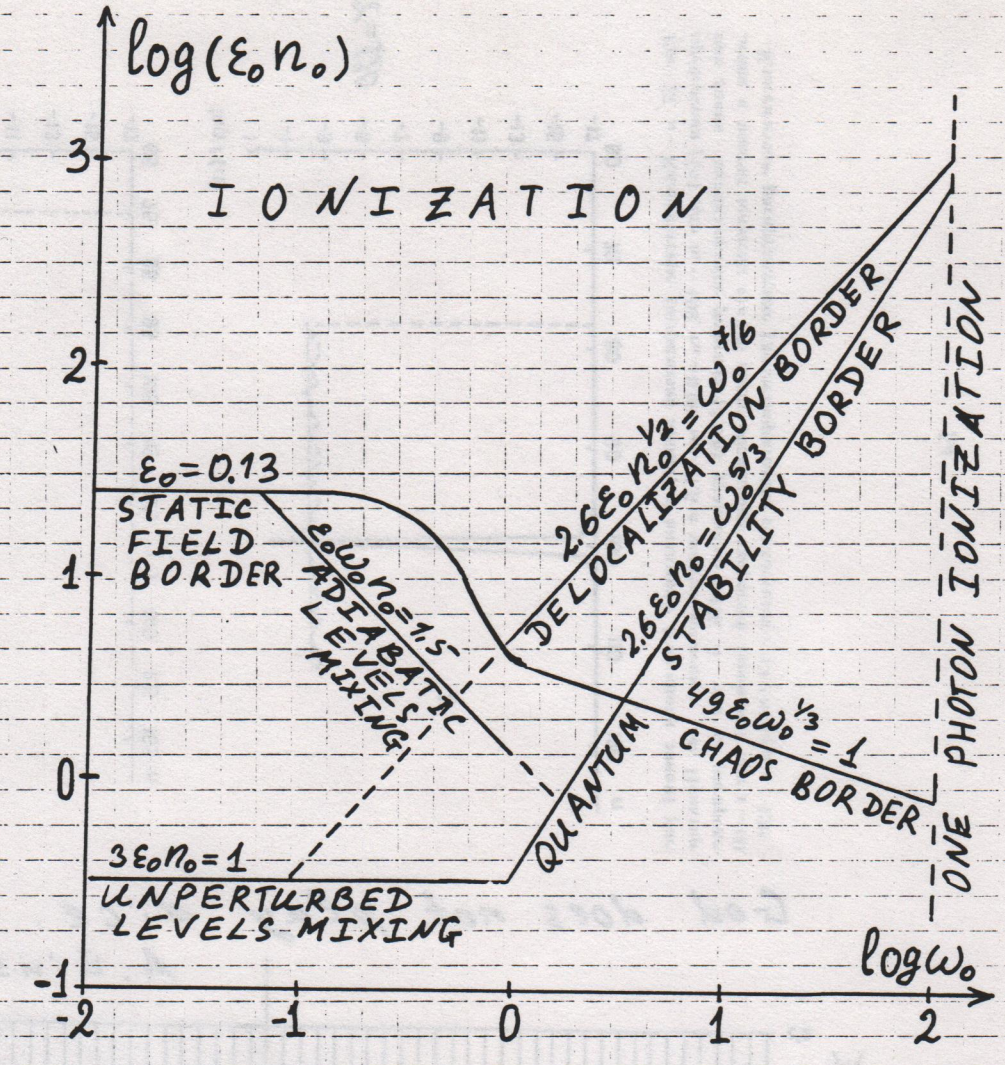


$n_0 = 200$

$V \sim \varepsilon n_0^2 \sim \varepsilon_0 n_0^{-2}$

$\Delta E = n_0^{-3}$

$\omega V \sim (\Delta E)^2$ — переход между адиабатическими уровнями